

## Assessment of Electricity Generation Using Medium-Temperature Geothermal Resources in Greece

Anastassios Stamatis<sup>1</sup>, Nikos Andritsos<sup>1</sup>

<sup>1</sup>Department of Mechanical Engineering, University of Thessaly, Pedion Areos, Volos, 38334, Greece

Email of A. Stamatis: [tastamat@uth.gr](mailto:tastamat@uth.gr)

**Keywords:** Power generation, Exergy analysis, Kalina cycle, Organic Rankine Cycle, Aspen Plus.

### ABSTRACT

This paper deals with a parametric investigation of two binary cycles that can be used for the exploitation medium temperature geothermal resources in Northern Greece. In order to perform such an investigation, models have been developed for a small KALINA (KCS34) power plant and for an Organic Rankine Cycle (ORC) one. The modelling was carried out using the Aspen Plus software. The models have been successfully validated with experimental data from two small commercial plants. The validated models were used to parametrically study plant performance for a typical range of climatic and geothermal conditions in a Greek geothermal field. The main parameters considered are the geothermal fluid temperature, ranging from 90 to 120 °C and the return temperature of the brine, which is assumed to be in the range of 70 - 80 °C.

### 1. INTRODUCTION

In Northern Greece and in some islands in the Aegean Sea there is a large number of low enthalpy geothermal fields with water temperatures of 30-90 °C. These fields are located at very shallow depths (typically 100-500 m) in the Tertiary sedimentary basins of North-eastern Greece (e.g. basins of Nestos River and Evros River) and in the islands of Samothrace, Chios and Lesvos (Fytikas and Kolios, 1992; Kolios et al., 2005; Kolios et al., 1997; Mendrinos et al., 2010).

The geological and tectonic conditions are favourable for the presence of medium enthalpy geothermal fields ( $T=90-130$  °C) at greater depths. In the area of Eratino-Chrysoupolis (Nestos River Delta), an area characterised by an elevated thermal gradient, two reservoirs have been identified. The first one is the main geothermal reservoir (high-enthalpy) and it is estimated to be lying at a depth of 1500 m. The Greek Public Petroleum Authority has measured 122 °C (in 1986) in a depth of 1377 m. The second one lies at a depth of 650-700 m. Heat is transferred from the main reservoir to the second one, where the geothermal fluid has a temperature of 70-80 °C.

Binary cycle energy conversion systems are successfully used to exploit low/medium temperature geothermal resources (e.g. Quick et al., 2013). They are usually constructed in small modular units and can be used efficiently for power generation for both off- and on-grid systems.

This scope of the paper aims is to parametrically analyse and assess known binary cycles suitable for the utilisation of low/medium enthalpy geothermal potential of in Northern Greece. In order to perform such an investigation, models for small power plant have been developed simulating a Kalina cycle (KCS34) or an Organic Rankine Cycle (ORC). The modeling for this work was performed using AspenPlus software. The KCS34 model has been successfully validated with data from two geothermal plants. The results of the simulation are very close to the actual site data.

After the validation step, the models were used to parametrically study the plant performance for the range of climatic and geothermal conditions in the area of Eratino-Chrysoupolis. The geothermal fluid inlet temperatures considered to be in the range 90–120 °C, while the return temperature of the brine is assumed to be between 70 and 80 °C.

Energy (and exergy) analysis of the plants is performed in order to define power production limits. Sensitivity analysis of the plants was also performed in order to identify the impact of main parameters such as ammonia mass fraction (KRS34) or the working fluid used (ORC), high cycle pressure and temperature on power, efficiency and size of the units.

### 2. BINARY CYCLES MODELLING

The first step in the parametric investigation of utilising low/medium temperature geothermal fluids for power generation is the development of appropriate models for a KALINA (KCS34) and an Organic Rankine Cycle (ORC) power plant. The latter cycle is used systematically with low and medium enthalpy sources, while the former one is considered to exhibit a higher thermal power output efficiency and it is used in a few geothermal sites.

Figure 1 shows a schematic diagram of the Kalina cycle process. Heat at a low temperature is transferred through a brine heat exchanger to a circulating mixture of ammonia and water. The ammonia–water mixture has a varying boiling and condensing temperature. During evaporation the mixing ratio of the binary working fluid changes because of the lower boiling temperature of ammonia. After the phase separator, the ammonia-rich steam passes through the turbine and a generator, coupled to the turbine, produces electricity. The saturated liquid from the separator is cooled down in a high temperature (HT) recuperator, where the sensible heat energy in this stream is used to preheat the feed stream to the evaporator. This liquid stream is then directed to the inlet of a low temperature (LT) recuperator, where it combines with the rich vapour exhaust from the turbine. The mixed-phase fluid is cooled down in a LT recuperator to preheat also the feed stream and it is condensed in the condenser.

Because of the change in the mixture ratio, the evaporation temperature increases continuously in the wet-steam region, whereas it decreases during condensation. Consequently, the process can be easily adapted to the relatively low temperature of the geothermal fluid under consideration and to the relatively high temperature of the cooling water, reducing the irreversibility in the heat exchange. The cycle constraints are dictated by the dew point of the mixture, that is when the boiling of the mixture is complete, and by the bubble temperature of the mixture, as it has to be lower or equal to the primary fluid outlet temperature to ensure a safe operation.

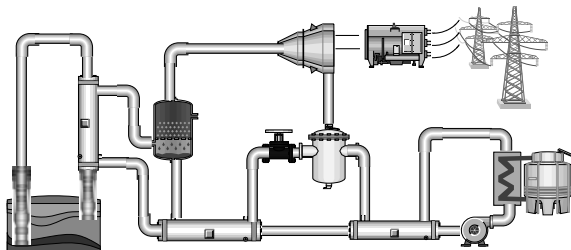


**Figure 1: Simplified schematic of the Kalina Cycle KCS34.**

The simple ORC is a basic Rankine cycle (Fig. 2), where a low boiling, organic substance is used as working medium instead of water. Due to the thermodynamic properties of the working medium, low-enthalpy resources can be used to generate electrical energy.

Several organic compounds have been used in ORCs to match the temperature of the available heat source. Organic substances generally have a higher molecular mass, leading to relatively small volume streams and to a compact size ORC unit. Another advantage of some organic compounds is that they do not need to be superheated, as with steam, as they do not form

liquid droplets upon expansion in the turbine. This prevents erosion of the turbine blades and provides design flexibility on the heat exchangers. However, in contrast to the Kalina cycle, the evaporation and condensing are realised taken place at constant temperatures giving ground to higher entropy generation.

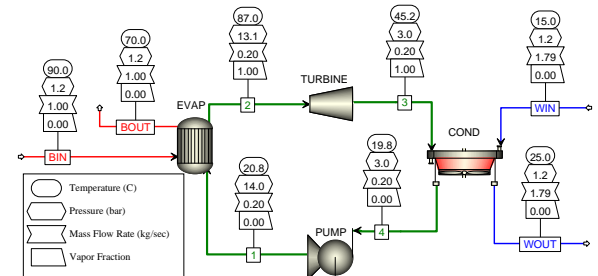


**Figure 2: Aspen Plus ORC model Flowsheet.**

The net power produced by the cycles,  $P_{NET}$ , is given by

$$P_{NET} = P_G - P_P \quad [1]$$

where  $P_G$  is the total power produced in the generator and  $P_P$  the total power consumed by the pump.

The thermal efficiency is defined as

$$\eta_{thermal} = \frac{P_{NET}}{Q_{BRINE}} = \frac{P_{NET}}{\dot{m}_{BRINE} \cdot (h_{BRINE,in} - h_{BRINE,out})} \quad [2]$$

where  $\dot{m}$  is the geothermal mass flow,  $h$  the enthalpy and  $Q$  the geothermal heat provided.

A more representative measure of plant performance is given by the exergetic efficiency defined as

$$\eta_{Ex} = \frac{P_{NET}}{Ex_{BRINE,in} - Ex_{BRINE,out}} \quad [3]$$

where  $Ex$  denotes available exergy.

The modelling for this work was implemented using Aspen Plus software. Aspen Plus provides a large number of databanks and methods for calculation of working media thermodynamic properties. It also provides built in blocks simulating the basic processes (such as pressure changers, heat exchangers, and separators) required for the modelling of the cycles.

In the following sections the modelling methodology of each component of the systems is described using the Aspen Plus terminology (words in *italics*). The Turbine and Pump are simulated in Aspen Plus using the *Compr* block defining the exit pressure and isentropic efficiencies. The evaporator, the condenser and the recuperators are simulated using the *HeatX* block with a shortcut calculation method selected. The blocks take into account the pressure losses in the two

streams. In the evaporator the hot stream temperature decrease is set, whereas in the condenser it is required that the vapour fraction at the exit is zero. Two more parameters are set; the hot exit-cold inlet temperature difference in the HT recuperator and the hot inlet-cold exit temperature difference in the LT recuperator. The Separator is simulated using the *Flash2* block without pressure drop and requiring zero heat duty. The *Mixer* and *Valve* blocks are used for the simulation of mixing and pressure control processes. Fig. 2 shows the ORC model developed in Aspen Plus.

### 2.1 KCS34 and ORC models validation

The Kalina and ORC models have been successfully validated with experimental data from two existing geothermal plants. The Husavik plant uses a KCS34 cycle with a mixture of 82% ammonia water (Mlcak et al., 2002). The water from the well in Husavik has a temperature of about 121 °C, considered as a medium enthalpy source, and it is cooled down to a

temperature suitable to the district heating system (80 °C). The installed capacity of the plant is about 1.7 MWe. Chena plant exploits a low enthalpy geothermal source to produce 210 kW power using a basic ORC cycle with R134a as working fluid (Aneke et al., 2011). In both plants the condenser is fed with a water of 5 °C. The results of the simulation, presented for both cases in Table 1, are in close agreement with available data from the existing plants found in the literature.

### 3. ASSESSMENT SETUP

After the validation step, the models were used to investigate a power plant performance for the range of climatic and geothermal conditions in the field of Eratino-Chrysoupolis. The geothermal fluid inlet temperatures is considered to be in the range of 90–120 °C, while the return temperature of the brine is assumed to be between 70 and 80 °C. Three different cases have been considered, as presented in Table 2.

**Table 1: Validation of KCS34 and ORC models with Husavik and Chena Geothermal Power Plants data (in *Italics* data used as input).**

Parameter	Husavik plant data	KCS34 Model	% error	Chena plant data	ORC model	% error
Working Fluid	NH <sub>3</sub> -Water	<i>NH3-Water</i>	-	<i>R134a</i>	<i>R134a</i>	-
Geothermal fluid mass flowrate (kg/s)	90	90	0	33.39	33.39	0
Geothermal fluid temperature (°C)	122	122	0	73.33	73.33	0
Geothermal exit temperature (°C)	80	80	0	54.44	54.44	0
Cooling water mass flowrate (kg/s)	182	182	0	101.68	102.81	1.11
Cooling water source temperature (°C)	4	4	0	4.44	4.44	0
Cooling water exit temperature (°C)	-	23	0	10	10	0
Turbine efficiency	-	0.73	0	0.80	0.8	0
Turbine inlet pressure (bar)	32.3	32.3	0	16.00	16	0
Turbine outlet pressure (bar)	6.6	6.6	0	4.39	4.39	0
Gross generator power (kW)	1823	1834	0.6	250.00	249.74	-0.1
Pump power (kW)	127	127.7	0.55	40.00	40.00	0
Working fluid mass flowrate (kg/s)	16.3	16.22	-0.49	12.17	12.24	0.57
Net plant power (kW)	1696	1707	0.64	210	209.74	-0.12
Thermal efficiency	-	10.78	-	0.08	0.0795	-0.62
Evaporator heat transfer rate (kWth)	-	15880	-	2580	2640	2.32
Condenser heat transfer rate (kWth)	-	14072	-	2360	2400	1.69

**Table 2: Representative Cases.**

CASE	A	B	C
Brine inlet temp. (°C)	120	105	90
Brine exit temp. (°C)	80	75	70
Cooling water source temp. (°C)	15	15	15
Cooling water exit temp. (°C)	20	20	20
Condensing temp. (°C)	25	25	25

Case A is representative of the maximum available heat when the brine exit temperature is maintained at a temperature appropriate for district heating applications. Case C represents the available heat at the minimum well temperature when the brine is re-injected at the lowest possible temperature of the

second well. Finally, Case B corresponds to the average temperature of the production and reinjection wells. For all the cases the following reasonable additional hypotheses have been made: Cooling water inlet temperature 15 °C (mean for the area of Eratino), cooling water exit temperature 20 °C and condensing temperature 25 °C.

The calculations are carried out using the models described previously with the following additional typical assumptions: isentropic efficiency of turbine 0.8, pump efficiency 0.7, electric generator and alternator efficiency 0.95, and minimum temperature difference in the recuperators 5 °C.

The varying parameters needed for the cycle's calculation, when the above parameters are fixed, are the turbine inlet pressure and temperature and the ammonia mass fraction for the KCS34 plant or the organic fluid used in the ORC plant. The limitations for the pressure and temperature are imposed by the minimum pinch temperature in heat exchangers, the bubble and dew temperature of the working fluid.

The potential of a plant for electricity generation is usually evaluated with respect to the net power, and to the thermal and exergetic efficiency (Nasruddin et al. 2009; Roy and Misra 2012). In this study, some additional criteria for the assessment of plant performance have been considered:

- The working mass flow  $\dot{m}_{wf}$  (indicative of the turbine and pump size for a given fluid).
- The total overall conductance,  $UA_{total}$ , i.e. the sum product of  $U$  and  $A$  for each heat exchanger, where  $U$  is the overall heat transfer coefficient and  $A$  is the cross-section area normal to the direction of heat transfer. This parameter is also related to the cost of the heat exchangers required to implement the plant. (Hettiarachchi et al., 2007)
- A total size indicator  $SI$  defined as:

$$SI = \dot{m}_{wf} \cdot UA_{total} \quad [4]$$

- A performance index,  $PI$ , expressing the power obtained for a given size:

$$PI = \frac{P_{NET}}{SI} \quad [5]$$

## 4. RESULTS

### 4.1 Kalina results

The ammonia mass fraction varied from 0.75 to 0.9. The results for four mass fraction values, namely 0.75, 0.8, 0.5, and 0.9, are presented in Figs 3 to 6. The different curves in Fig. 3 represent the net power, the total UA and the working fluid mass flow for four ammonia–water mixtures as a function of the turbine inlet pressure.

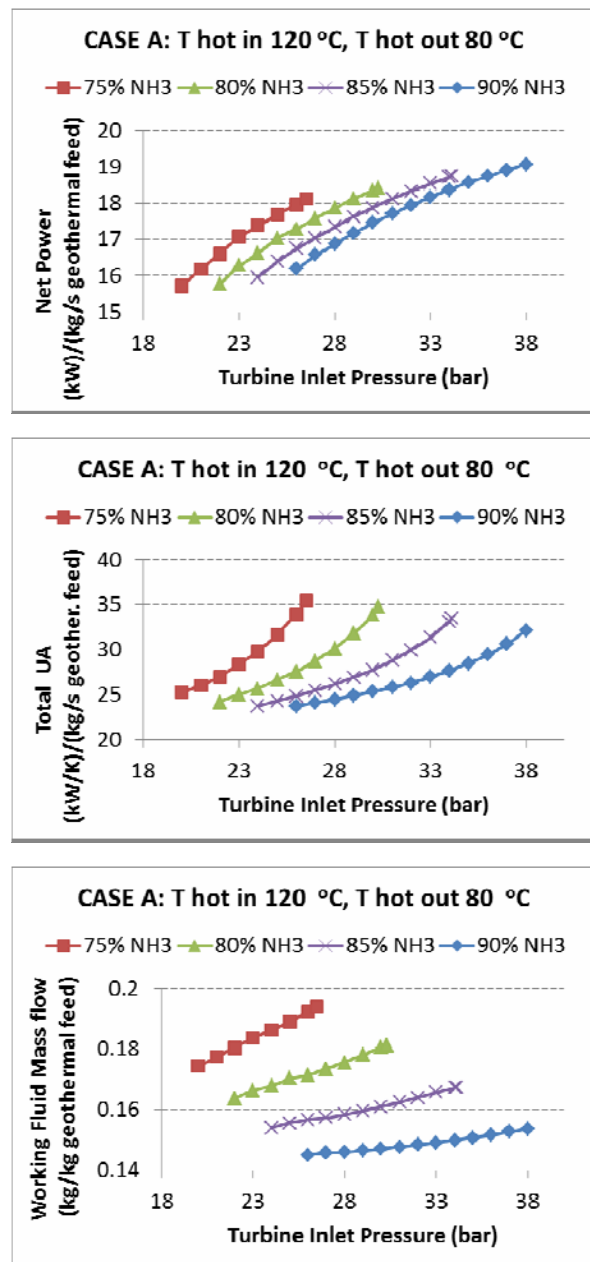
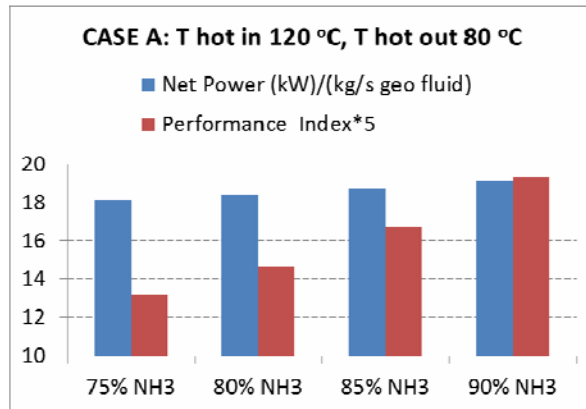


Figure 3: Results for the case A with a turbine inlet temperature of 115 °C.

The turbine inlet temperature has been fixed 5 °C lower than the hot inlet temperature, since, as it has been verified that for a given ammonia concentration and a given turbine inlet pressure, the lower the temperature the lower the net power produced. As expected, the power, the mass flow and the required heat exchanging area increase with increasing pressure. The opposite trend is observed regarding the mixture concentration for a given pressure. The higher the fractions of ammonia in the mixture, the lower are the power, the mass flow and the area. However, with increasing ammonia concentration the maximum allowable pressure increases and therefore the maximum power is obtained for the highest ammonia concentration.

Another interesting outcome of the analysis is evident when one considers the performance index associated

with the corresponding max power for each ammonia concentration, as clearly illustrated in Fig. 4. It is observed that increasing the ammonia mass fraction by 5% each time we obtain an increase of about 1.5-2% in max power, while the corresponding increase in the performance index is 10-15%. Both criteria indicate that the best choice for the case considered is the one having 90% NH<sub>3</sub> mass fraction at a maximum permissible pressure of 38 bars.



**Figure 4: Max net power and the corresponding performance cost index for various ammonia mass fractions.**

The maximum ammonia concentration (90%) in the analysis was imposed by the requirement that the liquid content of the mixture at the turbine exit is less than or equal to 5%. A condensation of more than 5% of the vapour at the turbine outlet seems unacceptable, since it could lead to erosion of the turbine blades. As illustrated in Fig. 5, increasing the pressure for a given ammonia concentration, the vapour fraction decreases, reaching a minimum at the maximum permissible pressure. As concentration increases, the minimum vapour fraction is getting lower reaching the 95% limit at 90% ammonia concentration.

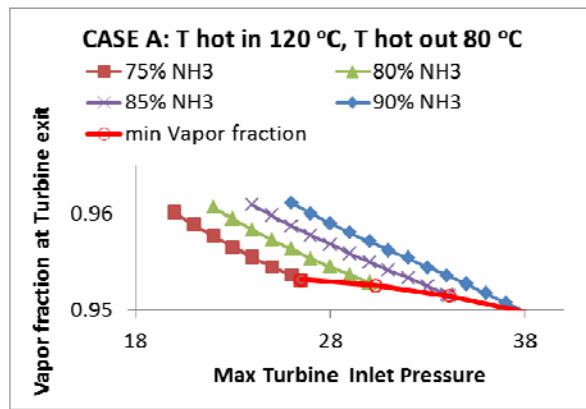


**Figure 5: Trend of vapour fraction at turbine exit as a function of Turbine Inlet pressure and ammonia concentration.**

Similar trends have been observed for cases B and C. A summary of the results are presented in Table 3.

**Table 3: KCS34 best results for the considered cases.**

Case	A	B	C
Max Net Power (kW)	19.06	12.57	7.25
Thermal Efficiency (%)	11.38	10.02	8.68
Exergy Efficiency (%)	50.13	48.64	47.24
UA (kW/K)	32.13	26.49	20.49
Mix. mass flow (Kg/s)	0.153	0.124	0.094
Evaporation pres. (bar)	38	33.1	28.7
Condens. pres. (bar)	8.68	8.68	8.68
Turbine Inlet Temp.(C)	115	100	85

As expected, more power is produced with increasing inlet temperature and inlet-outlet temperature difference of the brine. An interesting point here is observed in Figure 6. The performance index is almost constant, around 3.8, independent on the case considered, which indicates that the equipment size per kW does not change appreciably with the plant size.

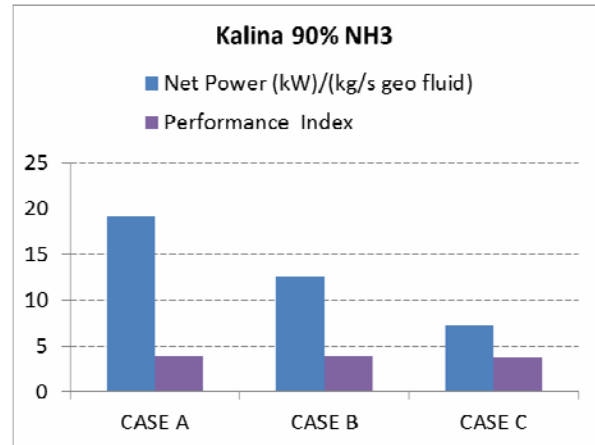


**Figure 6: Max power and the corresponding performance cost index for the three cases considered.**

#### 4.2 ORC results

Seven organic fluids, namely R134a, R123, R236ea, R245fa, R123, isobutene (R600a), propane (R290) and n-pentane (R601), with different characteristics have been assessed in this study. Their properties are shown in Table 4. (Chen et al., 2010). Their boiling points range from -42 to 36°C and their molecular weights from 58 to 153. Critical temperature ranges from 96 to 197°C, while critical pressure from 33 to 40 bars. Most of them (R123, R236ea, R245fa, R600a, and R601) are dry fluids, whereas R134a, and propane are wet fluids.

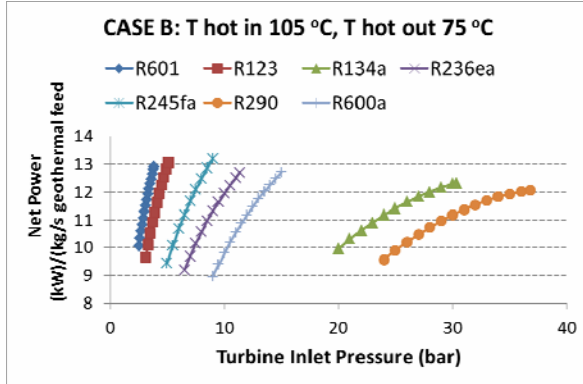
Once the working fluid has been selected the parameters needed for the cycle's determination, when the rest of the parameters considered are fixed, are the turbine inlet pressure and temperature. The limitations for the pressure and temperature are imposed by the minimum pinch temperature in heat

exchangers, and the bubble and dew temperature of the working fluid.

**Table 4: Working fluids properties.**

Fluid	Mol. weight	Boil. P (C)	T <sub>c</sub> (K)	P <sub>c</sub> (MPa)	Type
R123	152.9	27.8	183.6	3.66	Dry
R134a	102.0	-26.1	101	4.06	Wet
R236ea	152.0	6.5	139.3	3.50	Dry
R245fa	134.0	15.1	154	3.64	Dry
R290	44.10	-42.08	96.65	4.25	Wet
R600a	58.12	-11.7	134.6	3.63	Dry
R601	72.15	36.1	196.5	3.37	Dry

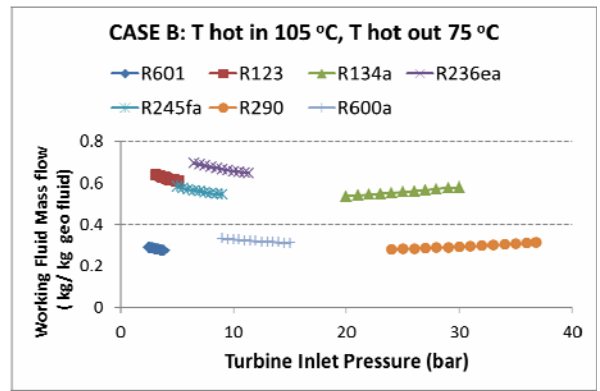
Figure 7 illustrates the net power produced for the various fluids considered as a function of the turbine inlet pressure. The turbine inlet temperature has been fixed at 5 °C lower than the hot inlet temperature for the wet fluids (R134a and R290), as it has been verified that a lower net power is produced at lower temperature for a specific turbine inlet pressure. For the dry fluids the turbine inlet temperature is the saturation temperature for that pressure. It was also verified for these fluids that this approach appears to be more effective than the one with a fixed temperature (Dai et al. 2009). As can be expected, the power increases with increasing pressure. Accordingly, the maximum power for each fluid is obtained at the maximum permissible pressure for a given condensation temperature, brine inlet and exit temperature and minimum temperature allowed.



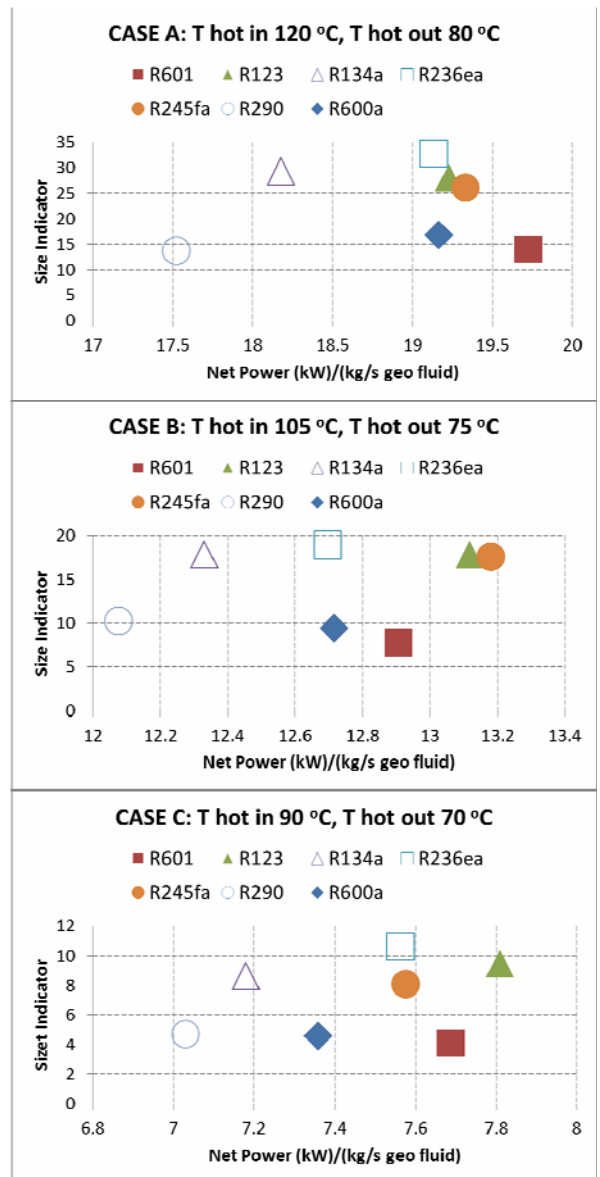
**Figure 7: Power vs turbine inlet pressure for the various fluids.**

Figure 8 demonstrates that the required working fluid mass flow rate is smaller for the lighter fluids (the fluids with smaller molecular weight). It is also evident that there is an opposite trend for the wet and dry fluids. By increasing the pressure, the mass flow for the dry fluids decreases, whereas it increases slightly for the wet fluids.

A more complete picture for the cases investigated is given in Fig 9, where the max power obtained for each fluid is given along with its associated size indicator.



**Figure 8: Mass flow vs Turbine Inlet Pressure for the various fluids.**



**Figure 9: Power vs Cost Indicator for the various fluids.**

It can be observed that, in general, the fluids to produce more power are the dry ones, with the highest boiling point among the tested fluids (R123, R601,

R245fa). This observation is similar to the one of Mago et al., 2007). On the other hand, the fluids with the worst efficiency are the wet ones having the lowest boiling point (R134a, R290). With regards to the size indicator (which should be understood as a comparison metric only for the same fluid), it can be seen that it is related to the molecular weight of the fluids. The lighter fluids (R601, R600a, and R290) exhibit the smaller size indicator. The ranking of the fluids for the three cases considered appears to change for the maximum power produced. R601 gives the highest power in CASE A, R245fa in CASE B and R123 in CASE C.

#### 4.3 Comparison of Kalina and ORC

A comparison of the two cycles with the optimum results is given in Table 5. It is noted that the results correspond to the maximum power generation target and the parameters (except the efficiencies) refer to 1 kg/s brine mass flow.

**Table 5: Cases best results for ORC &KCS34.**

	ORC	KCS34	% Rel. Diff.
<b>CASE C</b>			
Working fluid	R601	90% NH <sub>3</sub>	
Max net power (kW)	19.72	19.06	3.46
Thermal efficiency (%)	11.73	11.38	3.07
Exergy efficiency (%)	51.68	50.13	3.09
Total UA(kW/K)	40	32.13	24.5
Work. fluid mass flow(kg/s)	0.35	0.1535	128
<b>CASE B</b>			
Working fluid	R245fa	90% NH <sub>3</sub>	
Max net power (kW)	13.18	12.57	4.85
Thermal efficiency (%)	10.47	10.02	4.49
Exergy efficiency (%)	50.8	48.64	4.44
Total UA (kW/K)	32.28	26.5	21.8
Work. fluid mass flow (kg/s)	0.543	0.1245	336
<b>CASE C</b>			
Working fluid	R123	90% NH <sub>3</sub>	
Max net power (kW)	7.81	7.25	7.72
Thermal efficiency (%)	9.30	8.68	7.14
Exergy efficiency (%)	50.64	47.2	7.28
Total UA (kW/K)	22.79	20.49	11.2
Work. fluid mass flow (kg/s)	0.416	0.094	342

It is evident that in all the cases, the ORC cycle outperforms the KCS34 one in terms of power and efficiency. The ORC advantage is clearer for the lowest geothermal temperatures considered (CASE C), where ORC produces about 8% more power than KCS34. However, in all cases the Kalina cycle

requires substantially smaller total UA and 2 to 4 times less working fluid mass flow. As these parameters are related to the size and cost of the plants, eventually the cycle selection should be accompanied by a detailed economic analysis, taking also into consideration environmental and safety aspects.

Nevertheless, depending on the analysed representative cases and assuming a realistic geothermal flow rate of about 100 kg/s, the electrical power that can be produced is between 700 kW and 2 MWe.

#### 5. CONCLUSIONS

This paper presents a parametric investigation and assessment of two binary cycles for power production using low/medium temperature geothermal resources in Greece. Models have been developed in an ASPENPlus environment to simulate a KALINA (KCS34) and an Organic Rankine Cycle (ORC) small power plant. The models have been successfully validated with experimental data from two existing plants. The validated models were used to parametrically study a plant performance for the range of climatic and geothermal conditions in the Eratino-Chrysoupolis geothermal field. The analysis has demonstrated that, in contrast to a general belief, ORC cycles with the appropriate fluids are more effective than the Kalina cycle. However, there is a strong indication that ORCs required size, and thus cost, is considerably higher. Eventually it results that for both technologies in the best case a power production of about 2 MW is expected.

#### REFERENCES

Aneke, M., Agnew, B., and Underwood, C.: Performance analysis of the Chena binary geothermal power plant, *Applied Thermal Engineering*, **31**, 2011, 1825-1832

Chen, H., Goswami, D.Y., and Stefanakos, E.K.: A review of thermodynamic cycles and working fluids for the conversion of low-grade heat, *Renewable and Sustainable Energy Reviews*, **14**, (2010), 3059-3067.

Dai, Y., Wang, J., Gao, L. Parametric optimization and comparative study of organic Rankine cycle (ORC) for low grade waste heat recovery, *Energy Conversion and Management*, **50**, (2009), 576-582.

Fytikas, M., and Kolios, N.: Geothermal exploration in the west of the Nestos delta, *Acta Vulcanologica, Marinelli Volume*, **2**, (1992), 237-246.

Kolios, N., Fytikas, M., Arvanitis, A., Andritsos, N. and Koutsinos, S.: Prospective medium-enthalpy geothermal resources in sedimentary basins of Northern Greece, *Proceedings of the European Geothermal Congress 2007*, Unterhaching, Germany, (2007), paper #258, 1-11.

Kolios, N., Koutsinos, S., Arvanitis, A. and Karydakis, G.: Geothermal Situation in Northeasten Greece, *Proceedings of the World Geothermal Congress 2005*, Antalya, Turkey, (2005), paper #2614, 1-14.

Madhawa Hettiarachchi, H.D., Golubovic, M., Worek, W.M., and Ikegami, Y.: Optimum design criteria for an Organic Rankine cycle using low-temperature geothermal heat sources, *Energy*, **32**, (2007), 1698-1706.

Mago, P.J., Chamra, L.M., and Somayaji, C.: Performance analysis of different working fluids for use in organic Rankine cycles, *Proceedings of the Institution of Mechanical Engineers, Part A: Journal of Power and Energy*, **221**, (2007), 255-263.

Mlcak, H.A., Mirolli, M., Hjartarson, H., Húsavíkur, O., Ralph, M., Notes from the north: a report on the debut year of the 2 MW Kalina cycle® geothermal power plant in Húsavík, Iceland. *Geothermal Res. Council Trans.* **26**, (2002), 715-718.

Nasruddin, Usvika, R., Rifaldi, M., Noor, A.: Energy and exergy analysis of Kalina cycle system (KCS) 34 with mass fraction ammonia-water mixture variation, *Journal of Mechanical Science and Technology*, **23**, (2009), 1871-1876.

Quick, H., Michael, J., Arslan, U., and Huber, H.: Geothermal application in low-enthalpy regions, *Renewable Energy*, **49**, (2013), 133-136.

Roy, J.P., Misra, A., Parametric optimization and performance analysis of a regenerative Organic Rankine Cycle using R-123 for waste heat recovery, *Energy*, **39**, (2012), 227-235.